Acta Cryst. (1983). B39, 421–426

Electron Diffraction Study of the Si_2Te_3 Structural Transformation

BY P. E. GREGORIADES, G. L. BLERIS AND J. STOEMENOS

Physics Department, University of Thessaloniki, Greece

(*Received* 21 *October* 1982; *accepted* 9 *March* 1983)

Abstract

Electron diffraction *in situ* observations of Si_2Te_3 single crystals reveal a structural transformation above 673 K. In the temperature range 673–723 K diffuse-intensity honeycomb patterns appear, strongly suggesting a short-range collective phenomenon. On the basis of the cluster approximation, possible short-range-order arrangements in agreement with the diffuse intensity are given. Above 723 K a new ordered two-dimensional phase is formed, which can be described by an ordered occupation by the Si atoms of $\frac{1}{4}$ of the tetrahedral voids in the h.c.p. anion sublattice. Deviations from stoichiometry of the form $Si_{1+x}Te_3$, where $0{\cdot}5 < x < 1$, do not affect the structure. This can be explained on the basis of the statistical occurrence of Si atoms in the Te sublattice. Thus, Si_2Te_3 should be characterized as a non-stoichiometric compound of considerable stoichiometric width.

1. Introduction

Solid compounds of the Si–Te system have been investigated with respect to composition and structure, sometimes with contradictory results, while the electrical, thermal and optical properties have been reported to be the same for crystals of various compositions; for example, see Weiss & Weiss (1953), Vennik & Callaerts (1965), Roberts & Lind (1970), Lambros & Economou (1973), Taketoshi, Yoshikawa & Hamano (1974). Nevertheless, the investigations of Bailey (1966) and Brebrick (1968) on the phase diagram of the Si–Te system have confirmed that Si_2Te_3 is the only stable compound. The structure of Si_2Te_3 was investigated later by Ploog, Stetter, Nowitzki & Schönherr (1976).

Differential thermal analysis of Si_2Te_3 crystals revealed a thermal effect near 673 K (Bailey, 1966). The electrical conductivity and the Seebeck coefficient also showed a sudden change at 673 K (Ziegler, Junker & Birkholz, 1976). These effects were attributed to a solid–solid phase transition.

The purpose of this paper is the investigation of these crystals using electron diffraction techniques in order to study *in situ* the possible phase transition which has been discussed above.

2. Crystallographic information of Si_2Te_3

Weiss & Weiss (1953) first described the structure of Si_2Te_3 as a CdI_2-type layer structure with lattice constants $a_0 = 4{\cdot}28$, $c_0 = 6{\cdot}71$ Å and space group $P\bar{3}m1$. Later, however, several investigations confirmed that the unit cell of $SiTe_2$ as proposed by Weiss & Weiss (1953) is only a subcell of Si_2Te_3. The structure of Si_2Te_3 belongs to the space group $P\bar{3}1c$ with lattice constants $a = 7{\cdot}429$ ($\sim\sqrt{3} \times 4{\cdot}289$ Å) and $c = 13{\cdot}471$ Å ($\sim 2 \times 6{\cdot}7$ Å) with $Z = 4$ (Ploog, Stetter, Nowitzki & Schönherr, 1976). The Te atoms form an h.c.p. lattice with the Si atoms arranged in pairs occupying $\frac{2}{3}$ of the octahedral voids in alternating (0001) planes (Fig. 1*a*). Therefore, the structure of Si_2Te_3 is a CdI_2-type derivative with only $\frac{2}{3}$ of the cation sites occupied in a layer of octahedral voids. Each Te atom is bonded to only two Si atoms in neighbouring octahedral sites with Si–Te–Si bond angles about 93°. Each Si atom is tetrahedrally coordinated by one Si and three Te atoms, with Si–Te and Si–Si bond distances of 2·55 and 2·3 Å, respectively (Fig. 1*b*). Only $\frac{1}{4}$ of the Si_2 units run parallel to the *c*-axis direction, the others exhibiting more complex orientations (Fig. 1*c*). If a_0 and c_0 are the lattice constants of the h.c.p. Te sublattice, then the unit cell of Si_2Te_3 may be described by the constants $a = a_0\sqrt{3}$ and $c = 2c_0$, and contains three octahedral voids designated by A, B, C with coordinates $A(0,0)$, $B(\frac{1}{3},\frac{2}{3})$ and $C(\frac{2}{3},\frac{1}{3})$ (Fig. 1*b*). Thus the occupied octahedra can be described by the sequence along the *c* axis $-\square-(A + B)-\square-(A + C)-\square-(B + C)-$ where A,B,C refer to occupied octahedral sites in a layer and $\square$ denotes the vacant octahedral layers. In this way the empty octahedral sites of the h.c.p. Te sublattice form a trigonal lattice. This structure offers a simple explanation for the non-metallic character of Si_2Te_3 which is due to the occurrence of Si pairs in $\frac{2}{3}$ of the octahedral sites of a CdI_2-type structure (Hulliger, 1976). The above coordination of the atoms is in agreement with the results of the amorphous material in the glass-forming region,

0108-7681/83/040421-06$01.50

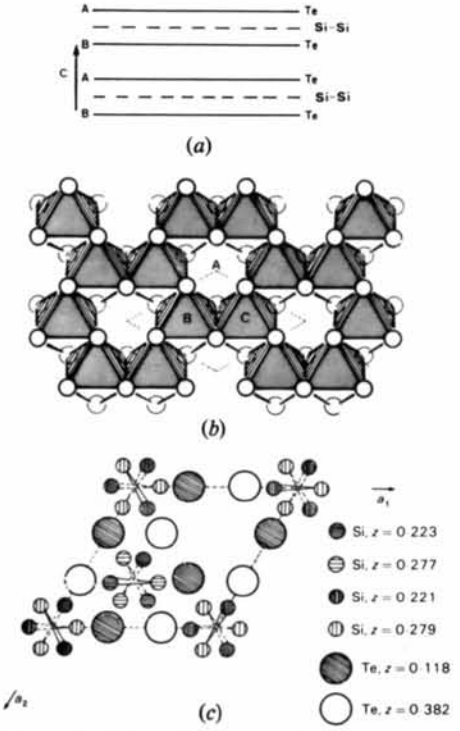

Fig. 1. (*a*) Successive layers of Te atoms in h.c.p. order along the *c* axis. The intermediate octahedral voids between two successive layers *AB* are $\frac{1}{3}$ filled by Si_2 units. (*b*) The octahedral sites between two successive layers of Te atoms. Te atoms in the upper layer are denoted by the heavy circles, and in the lower one with light circles. Only the shaded octahedra are occupied by Si pairs. (*c*) Projection of the Si_2Te_3 unit cell on the (0001) plane. All possible orientations of Si–Si pairs are shown. For clarity only half of the cell parallel to the *c* axis is projected.

15–25 at.% Si, of the Si–Te system (Petersen, Birkholz & Adler, 1973; Bartsch, Bromme & Just, 1975).

3. Crystal growth and specimen preparation

Si_2Te_3 single crystals of an adequate size were grown from commercially available 99·99% pure elements. The two components were placed in a quartz ampoule 10 cm long and 2 cm in diameter, and the ampoule was sealed under a vacuum of $1{\cdot}3 \times 10^{-3}$ Pa. The ampoule was placed in a vertical furnace with a linear temperature gradient starting from 1273 K. The quartz ampoule remained in the highest-temperature site for 24 h in order to achieve complete melt homogeneity. After 24 h the ampoule was lowered, by means of a suitable mechanism, at a lowering rate of 33 mm d^{-1} to the temperature of 1073 K. At this point the power of the furnace was turned off so that the ampoule was cooled slowly in about 10 h.

Single crystals prepared by this method were deep red with cleavage at the (0001) plane and were approximately 3 cm long and 2 cm wide. We performed X-ray-analysis, chemical-analysis, and DTA experiments to confirm the quality of the crystals.

The easy cleavage parallel to the (0001) planes allowed the preparation of thin specimens for TEM, using adhesive tape. A JEM 120CX electron microscope operating at 100 kV, equipped with a single-axis tilt ±60°, as well as a heating and cooling holder having a single-axis tilt ±45°, was used. A built-in liquid-N_2 anticontamination trap permits a very low specimen contamination rate of 0·1 Å min^{-1}.

4. Electron-microscopy study

Tilting experiments allowed the confirmation of the reciprocal lattice which corresponds to the structure reported by Ploog, Stetter, Nowitzki & Schönherr (1976) (Fig. 2). By heating and cooling the sample *in situ* we found that the intense spots, designated in Fig. 2 by large dots, remain unaltered in the temperature range 77 to 823 K. The weak spots designated in Fig. 2 by small dots are considered as 'superlattice' spots. We are justified in considering these spots as superlattice since they change during the heating of the specimen.

At 673 K, diffuse intensity was observed (Fig. 3*b*). The diffuse intensity was concentrated along a thick honeycomb pattern. Tilting experiments showed that the diffuse intensity along the c^* axis was very weak. Each superlattice spot in the $(0001)^*$ section was surrounded by a hexagon of diffuse intensity concentrated on the Brillouin-zone boundaries parallel to the $[0001]^*$ axis.

In some cases single crystals, produced as described in §3, showed diffuse scattering intensity without any additional heat process in the electron microscope except that which occurred during growth (Lambros & Economou, 1973).

Above 723 K the superlattice spots of $\frac{1}{3}\{11\bar{2}0\}$ type vanish and new weak spots of $\frac{1}{2}\{10\bar{1}0\}$ type appear (Fig. 4). In fact, these were not spots but streaks along the c^* axis, as can be deduced by tilting the specimen along the $[10\bar{1}0]^*$ axis. The tilting experiment was performed by tilting the specimen at a speed 60° min^{-1}, from an angle of 3° to the final angle of 38° (Fig. 5) while the camera diaphragm was held open through the

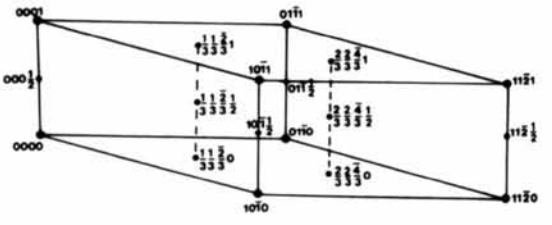

Fig. 2. Reciprocal lattice of the ordered Si_2Te_3.

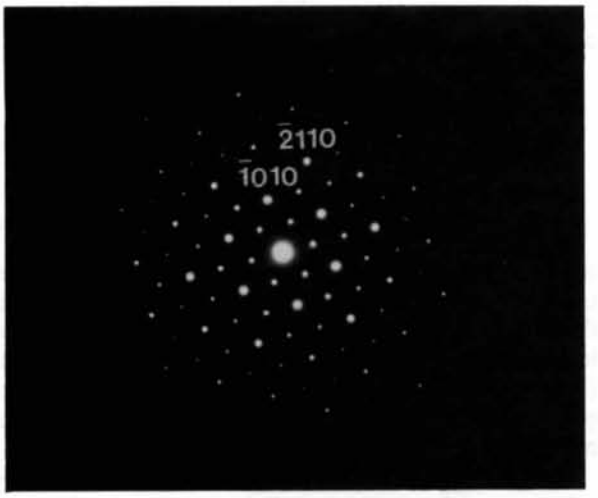

(*a*)

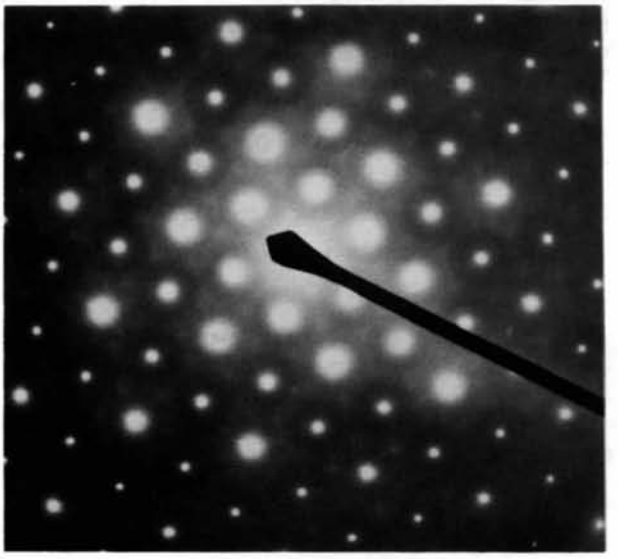

(*b*)

Fig. 3. (*a*) Diffraction patterns of (0001)* section of the ordered phase at room temperature. Only the basic spots are indexed. (*b*) Electron diffraction pattern showing diffuse scattering at 673 K, (0001)* section.

Fig. 4. Diffraction pattern at a temperature > 773 K, (0001)* section; weak pseudospots of $\frac{1}{2}\{10\bar{1}0\}$ type appear.

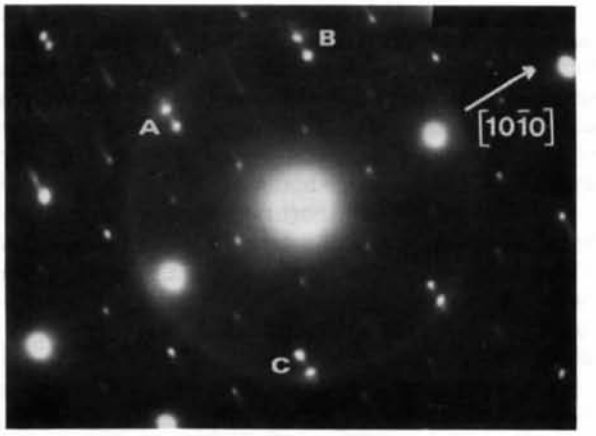

Fig. 5. The specimen tilted along the $[10\bar{1}0]^*$ axis during the exposure time. Note the streaks that appear instead of the $\frac{1}{2}\{10\bar{1}0\}$ spots.

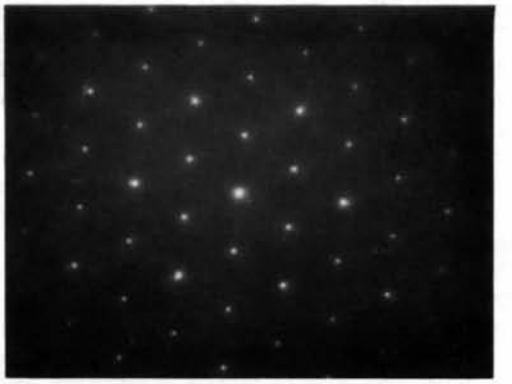

Fig. 6. Diffraction patterns from the (0001)* section where superlattice spots are absent.

whole experiment. The superlattice spots that do not lie on the tilting axis give an intensity distribution perpendicular to this axis, as the Ewald sphere intersects the streaks in reciprocal space along the *c* axis. The main spots of the $\{1\bar{1}00\}^*$ type do not show continuous intensity distribution perpendicular to the $[10\bar{1}0]^*$ axis but new spots appear that belong to a different Laue zone (spots *A*, *B*, *C* in Fig. 5). Finally, at about 823 K the (0001)* section shows only the intense spots, of the $\{1\bar{1}00\}$ type (Fig. 6). It is interesting that these diffraction patterns remain unaltered when the crystals are allowed to cool slowly from this temperature.

5. Analysis of the results

5.1. *Interpretation of the diffuse-intensity patterns*

The symmetrical honeycomb patterns of the diffuse intensity that were observed when the temperature was

raised above 673 K strongly suggest a short-range collective phenomenon. As long as the temperature remains close to 673 K the intensity of the superlattice spots, which describe the ordering of the Si–Si units, does not change and a possible explanation of the phenomenon may be given by considering a thermodynamical mean average break-up of some of the Si–Si units. The study of this short-range rearrangement may be made on the basis of a ternary system $(A\square)_{1-x}B_x$ where a new ordering process takes place in the sublattice of Si_2 units and the remaining octahedral vacant $\square$ sites. The extension of a binary system to a ternary hypothetical one, where the third participant is a set of vacant sites, into which some of the atoms of the compound may migrate, is a model which has been proved very useful (Karakostas, Flevaris, Vlachavas, Bleris & Economou, 1978).

In our case the geometry of the $(Si_2\square)_{1-x}$ sublattice is shown in Fig. 1(*b*) where in each layer of octahedral interstices the three nonequivalent sites marked by *A*, *B*, *C* are only $\frac{2}{3}$ filled by Si_2 units in an ordered way.

Upon heating the crystal it is expected that the Si_2 units will start to break up at random into two silicon ions, which cannot be accommodated in the same octahedral interstices. Thus, to a first approximation we can expect an average distribution of ions into clusters, the correlation between them being destroyed with the raising of the temperature.

There are six tetrahedra and two octahedra sharing common faces with an octahedron initially containing an Si_2 unit. The six tetrahedra lie in the same double layer of Te atoms (Fig. 7*a*) surrounding the central octahedron. The six tetrahedral can be grouped into two sets of three, whose centres lie in two different planes at a distance $\pm c_0/8$ from the plane of the octahedral interstices (Fig. 7*b*). One set of tetrahedra points downwards while the other set points upwards. The distances between the centres of a tetrahedron–central octahedron (*AB* in Fig. 7*b*) and octahedron–central octahedron (*BC* in Fig. 7*b*) are correspondingly:

$$(AB) = \left[\left(\frac{c_0}{8}\right)^2 + \left(\frac{a_0}{\sqrt{3}}\right)^2\right]^{1/2} = 2{\cdot}61 \text{ Å and}$$

$$(CB) = \frac{c_0}{2} = 3{\cdot}37 \text{ Å},$$

where $a_0 = 4{\cdot}289$ and $c_0 = 6{\cdot}74$ Å (the unit-cell constants for Te sublattice). Therefore, one may expect the silicon ions to shift preferentially to the neighbouring tetrahedral sites. The orientations of the Si_2 units (Fig. 1*c*) are also such as to make the above distance even smaller. In this way the Si tetrahedral coordination is preserved.

This phenomenological discussion does not give any information about the sort of clusters that the Si atoms form at the tetrahedral sites. In order to obtain information about the type of clusters that occur, the cluster theory developed by De Ridder, Van Tendeloo, Van Dyck & Amelinckx (1976) can be applied.

The honeycomb pattern (Fig. 8*a*) can be described by the combination of two simple diffuse patterns (Fig. 8*b*, *c*) and their locus can be described by the equation

$$\begin{aligned}\omega_0 = {} & 2\omega_1[\cos 2\pi h + \cos 2\pi k + \cos 2\pi(h+k)] \\ & + 2\omega_2[\cos 2\pi(2h+k) + \cos 2\pi(2k+h) \\ & + \cos 2\pi(h-k)],\end{aligned} \tag{1}$$

where the values of the parameters $(\omega_0,\omega_1,\omega_2)$ are (18,8,1) and (22,10,1) respectively (Van Goethem, De Ridder, Van Dyck & Amelinckx, 1979).

It has already been proved that equation (1) monotonically related to a cluster relation of the form

$$\omega_o \bar{\sigma}_0 + \omega_1 \sum_1 \bar{\sigma}_1 + \omega_2 \sum_2 \bar{\sigma}_2 = 0 \tag{2}$$

describes a hexagonal thirteen-point cluster composed of a central atom surrounded by six first-nearest and six second-nearest neighbours.

Since the number of atoms that are involved in the cluster is large we could build numerous clusters that satisfy relation (2). From this, two pairs of clusters described in Fig. 9(*a*, *b*) are particularly important. According to the goodness criterion (Van Dyck, De

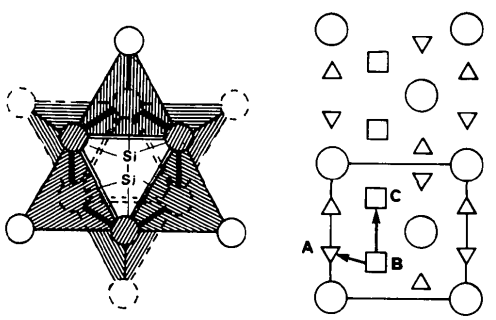

(*a*) (*b*)

Fig. 7. (*a*) The octahedron between two successive layers of Te atoms is surrounded by six tetrahedra which are in the same double layer of Te atoms. (*b*) Interstices in the h.c.p. arrangement, projection on the (11$\bar{2}$0) plane. Tetrahedral interstices are denoted by ∇ or $\triangle$, octahedral ones by $\square$.

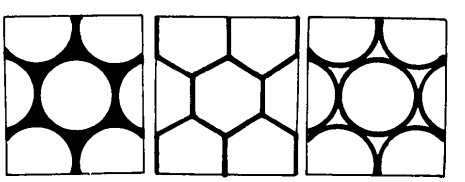

(*a*) (*b*) (*c*)

Fig. 8. (*a*) The honeycomb pattern of the diffuse intensity of Fig. 3(*b*) can be composed by two diffuse intensity loci (*b*) and (*c*).

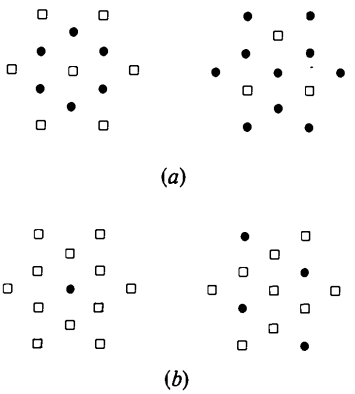

Fig. 9. The two possible pairs of clusters (*a*) and (*b*).

Ridder, Van Tendeloo & Amelinckx, 1977) these clusters satisfy relation (2) quite well. The first pair of clusters (Fig. 9*a*) consists of the fundamental unit of the structure Si_2Te_3. This entails a short-range order of the Si_2 pairs and the vacant octahedral sites, and explains the break-up of the Si_2 pairs.

The second pair of clusters (Fig. 9*b*) form the basic structural units of a $2a_0$-type structure which gives diffraction patterns similar to those observed when the sample was heated above 723 K.

Therefore, the spontaneous appearance of diffuse intensity in a narrow range of temperature corresponds to a statistical break-up of the Si_2 pairs and the Si atoms migrate in new vacant tetrahedral sites that are responsible for the superlattice spots of $(\frac{1}{2}00)$ type as we shall see in §5.2. These spots correspond to places of minimum potential energy (Zhorovkov, Fuks & Panin, 1975).

5.2. *The high-temperature superstructure*

The presence of streaks of $\frac{1}{2}\{10\bar{1}0\}$ type along the c^* axis above 723 K can be attributed to a two-dimensional superlattice with constant $a' = 2a_0$, where a_0 is the lattice constant of the Te sublattice in the basal plane while the crystal was highly disordered along the c axis. The Te sublattice remains unaltered but all the Si_2 units break up and silicon ions occupy the neighbouring tetrahedral sites in a double layer of Te atoms. Fig. 10(*a*) shows the arrangement of occupied tetrahedral sites in the double layer of Te atoms which can lead to a two-dimensional lattice with constant $a' = 2a_0$ which is consistent with the superlattice diffraction patterns of $\frac{1}{2}\{10\bar{1}0\}$ type (Fig. 4). In Fig. 10(*a*) the tetrahedral sites with coordinates $(0,0,\frac{3}{8})$ occupied by silicon ions are denoted with full circles while those occupied with coordinates $(\frac{2}{3},\frac{1}{3},\frac{1}{8})$ are denoted with open circles. In both sets of tetrahedral sites the occupation distribution of Si atoms is the same. Fig. 10(*b*) shows the arrangement of the

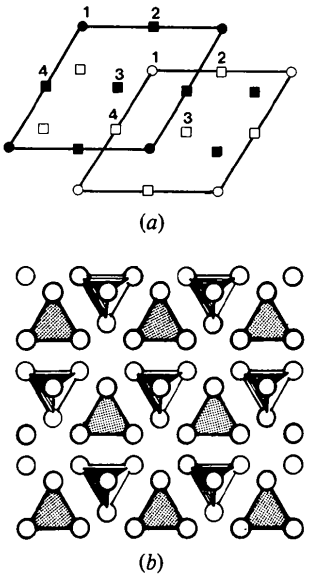

Fig. 10. (*a*) Relative positions of the two sublattices formed by the tetrahedra. (*b*) Arrangement of the tetrahedra occupied by Si atoms in a layer.

tetrahedra occupied by Si atoms in a sandwich of two Te layers.

The ordered arrangement of the Si atoms in $\frac{1}{4}$ of all the tetrahedral sites of the h.c.p. Te sublattice leads to the sequence

$$A\beta_{1/4}\,\alpha_{1/4}\,B\alpha_{1/4}\,\beta_{1/4}\,A\beta_{1/4}\ldots$$

where $\ldots ABA\ldots$ is the h.c.p. sequence of Te atoms and $\ldots\alpha\beta\alpha\ldots$ represents tetrahedral voids. The streaks along the c^* axis should be attributed to stacking faults, *i.e.* loss of correlation between different double layers.

In this way the Si atoms take up only $\frac{1}{4}$ of the sites of each tetrahedral sublattice. Each Te atom is bonded to only two Si atoms in the tetrahedra above or below the Te layers, while the coordination of the atoms is retained; *i.e.* the Si atoms remain tetravalent and the Te atoms divalent. Each unit cell contains two Te atoms, four tetrahedral interstices and two octahedral ones. Each octahedral site corresponds to two neighbouring tetrahedral ones which could be occupied by silicon ions. Only half of them are occupied (Fig. 10). In other words, only $\frac{1}{4}$ of all the tetrahedral sites are occupied, *i.e.* [four tetrahedral interstices] $\times$ $\frac{1}{4}$ Si atoms correspond to two Te atoms per unit cell leading to the stoichiometric composition $SiTe_2$ or, better, $Si_{1.5}Te_3$. This means that some of the Si atoms should be intercalated in the van der Waals region. This deviation from stoichiometry is probably one reason that no superlattice spots of $\frac{1}{3}\{11\bar{2}0\}$ type appear again if the crystals are allowed to cool slowly in the electron microscope. Moreover, at 823 K all the superlattice

spots disappear revealing the existence of a state of completely disordered Si atoms in the Te sublattice, while the basic spots of the Te sublattice remain invariant.

6. Discussion and conclusions

TEM observation revealed that near 673 K a phase transition takes place, which is accompanied by a periodic diffuse-intensity locus in reciprocal space (Fig. 3*b*). This was attributed to a short-range state which was interpreted in terms of a cluster model where a new ordering process takes place in the sublattice of Si_2 units and the remaining octahedral vacant □ sites. As the temperature increases the diffuse patterns evolve to distinct streaks of $\frac{1}{2}\{10\bar{1}0\}$ type along the c^* axis. On the assumption that the Te sublattice and the co-ordination of the atoms are also retained, these diffraction data may be attributed to the complete break-up of the Si_2 units and to the occupation of all the available tetrahedral sites in the double layers of the Te atoms by the silicon ions. In this case $\frac{1}{4}$ of Si atoms should be intercalated in the van der Waals gap while the loss of correlation in the successive layers of Te leads to a two-dimensional superlattice with the stoichiometric composition $Si_{1.5}Te_3$. The phenomenon was not reversible when the crystal was allowed to cool, probably because of the open thermodynamic prevailing in the electron microscope.

Any attempt to grow crystals of varying stoichiometry with the nominal composition $Si_{1+x}Te_3$ where $0 < x < 1$ with the method we have described in §3 gave single crystals whose chemical analysis showed stoichiometric compositions $Si_{1+x}Te_3$ ranging from $0{\cdot}5 < x < 1$, $Si_{1.5}Te_3$ (=$SiTe_2$), to Si_2Te_3. All these crystals have the same crystallographic data, as well as optical and electrical properties, as those of Si_2Te_3 which reveals that Si_2Te_3 is a non-stoichiometric compound of considerable width (Ziegler, 1976) in which a percentage of Si–Si pairs is allowed statistically to be missing. This is also the case for other compounds of the Group IV transition-metal dichalcogenides (Lieth & Terhell, 1977).

We would like to thank Professor K. Alexiadis, director of the Laboratory of Analytical Chemistry of the Chemical Engineering Department, for the chemical analysis of the crystals.

References

BAILEY, L. G. (1966). *J. Phys. Chem. Solids*, **27**, 1593–1598.

BARTSCH, G. E. A., BROMME, H. & JUST, T. (1975). *J. Non-Cryst. Solids*, **18**, 65–75.

BREBRICK, R. F. (1968). *J. Chem. Phys.* **49**, 2584–2592.

DE RIDDER, R., VAN TENDELOO, G., VAN DYCK, D. & AMELINCKX, S. (1976). *Phys. Status Solidi A*, **38**, 663–674.

HULLIGER, F. (1976). *Structural Chemistry of Layer-Type Phases*, edited by F. LEVY, pp. 151–152. Dordrecht, Holland/Boston, USA: Reidel.

KARAKOSTAS, TH., FLEVARIS, N. F., VLACHAVAS, N., BLERIS, G. L. & ECONOMOU, N. A. (1978). *Acta Cryst.* A**34**, 123–126.

LAMBROS, A. P. & ECONOMOU, N. A. (1973). *Phys. Status Solidi B*, **57**, 793–799.

LIETH, R. M. A. & TERHELL, J. G. J. M. (1977). *Preparation and Crystal Growth of Materials with Layered Structures*, pp. 162–163. Dordrecht, Holland/Boston, USA: Reidel.

PETERSEN, K. E., BIRKHOLZ, U. & ADLER, D. (1973). *Phys. Rev. B*, **8**, 1453–1460.

PLOOG, K., STETTER, W., NOWITZKI, A. & SCHÖNHERR, E. (1976). *Mater. Res. Bull.* **11**, 1147–1154.

ROBERTS, G. G. & LIND, E. L. (1970). *Phys. Lett. A*, **33**, 365–366.

TAKETOSHI, K., YOSHIKAWA, S. & HAMANO, K. (1974). *NHK (Nippon Hoso Kyokai) Tech. J.* **26**, 172–178.

VAN DYCK, D., DE RIDDER, R., VAN TENDELOO, G. & AMELINCKX, S. (1977). *Phys. Status Solidi A*, **43**, 541–552.

VAN GOETHEM, L., DE RIDDER, R., VAN DYCK, D. & AMELINCKX, S. (1979). *Phys. Status Solidi A*, **55**, 67–77.

VENNIK, J. & CALLAERTS, R. (1965). *C. R. Acad. Sci.* **260**, 496–499.

WEISS, A. & WEISS, A. (1953). *Z. Anorg. Allg. Chem.* **273**, 124–128.

ZHOROVKOV, M. F., FUKS, D. L. & PANIN, V. E. (1975). *Phys. Status Solidi B*, **68**, 379–385.

ZIEGLER, K. (1976). *Elektronische Eigenschaften von* Si_2Te_3 *Einkristallen*. Dipl.-Phys., Karlsruhe, pp. 5–6.

ZIEGLER, K., JUNKER, H. & BIRKHOLZ, U. (1976). *Phys. Status Solidi A*, **37**, K97.